Extending Application of Simple for Dead and Continuous for Live Load Steel Bridge System to ABC Applications in Seismic Regions- Phase II- Experimental

Submitted by
Amir Sadeghnejad

FINAL REPORT

Department of Civil and Environmental Engineering
Florida International University
Miami, Florida

Submitted to
Atorod Azizinamini
Director, ABC-UTC
June 2018
ABC-UTC

Contents

Abstract

Simple for Dead load and Continuous for Live load (SDCL) steel bridge system has proven to be economical for non-seismic application. Although the system has been used in different methods of construction, this paper concentrates on Accelerated Bridge Construction (ABC) application. The application of the SDCL steel bridge system in high seismic areas has been nonexistent, mainly due to lack of appropriate details. The extension of the SDCL system to high seismic areas was initiated by conducting detailed numerical analysis to comprehend types of forces that the connection must resist. The results of the numerical study lead to development of connection details over middle pier. Thereafter, a component testing of the proposed SDCL connection was carried out to find the ultimate limit states, verification of numerical results, and merits of the proposed detail in light of established seismic design provisions. The developed connection behaved as designed and prevented damage to capacity protected elements. The column showed sufficient ductility during cyclic tests, which indicated the connection will perform well under high levels of displacement.

Introduction and Background

Non-seismic Simple for Dead Load and Continuous for Live Load (SDCL)

Simple for Dead load and Continuous for Live load (SDCL) steel bridge system has been used in conventional and accelerated construction methods of building bridges, mainly in non-seismic areas. The SDCL steel bridge system for non-seismic areas was developed at the University of Nebraska-Lincoln (Azizinamini, Yakel, and Farimani 2005). The SDCL system is providing new opportunities for developing economical multi-span steel bridge systems. The SDCL system is especially well suited for multi-span bridges with each span having maximum length of about 250 ft. Complete summary of research, application, and performance of the SDCL steel bridge system, as applied to non-seismic areas, using conventional and Accelerated Bridge Construction (ABC) methods of construction, is provided elsewhere (Lampe et al. 2014; Azizinamini 2014; Farimani et al. 2014; Yakel and Azizinamini 2014; Javidi, Yakel, and Azizinamini 2014). A brief introduction of the SDCL system follows. For a detailed description of the system, refer to the references cited above.

Figure 1 shows construction details of a conventional two-span continuous steel bridge girder. For continuity over a pier, the middle segment of the steel girder is placed and then connected to end segments with either a bolted or welded field splice. The launching and placement of end segments usually requires two cranes on site with possible traffic interruptions. In the SDCL system, for example, for a two span bridge, girders are placed over the abutment and pier and joined together over the middle pier using concrete diaphragm. Figure 2 shows a schematic of an SDCL system.

There are different approaches to constructing bridges using ABC. One of these approaches is the modular approach, in which the contributory width of the deck is cast on top of the girders and shipped to final site. These modular units are then joined together using longitudinal closure joints. The SDCL steel bridge system is well suited for these types of ABC projects. Figure 3 shows schematically the ABC application of SDCL in non-seismic regions (Javidi, S., Yakel, A., and Azizinamini, A., 2014).

ABC application of an SDCL steel bridge system has many advantages including eliminating bolted splices, eliminating joints, reduced negative moment over the pier, and minimized traffic interruption. Further, encasing the ends of the girder in concrete protects the girder ends and results in enhanced service life and lower inspection and maintenance costs as compared to conventional steel bridge systems. Until now the application of an SDCL steel bridge system in high seismic areas has been nonexistent, due to lack of details suitable for seismic regions. As ABC applications are becoming more popular in bridge construction, there is a need for a suitable detail of the SDCL steel bridge system in seismic areas.

Following is one approach for construction of an SDCL steel bridge system using ABC. The process is shown schematically in Figure 4. The first step is to place a dropped cap beam over the precast columns. The purpose of the dropped cap beam is to allow support of steel girders with deck cast on top. The next step is to attach the modules (steel deck plus the deck) using longitudinal closure joints and transverse joint (diaphragm) over the support. The key design item is the type of detail that should be used to join the modules over the pier.

The focus of this paper is to suggest such detail and, using an experimental test, verify its merits. The extension of the SDCL steel bridge system to high seismic areas was initiated by conducting detailed numerical analysis that aided in comprehending the types of forces that connection detail over middle piers, where girders are joined together, must resist in high seismic areas. The end result was the development of detail for connecting the girders over middle pier and making them integral with bridge columns. The next section provides an overview of the suggested detail for connecting the modules over the pier.

Development of Detail for Use of SDCL System in High Seismic Areas

The design philosophy for bridges in seismic areas is to predefine locations for damage and design them for adequate levels of ductility. In this design approach, the superstructure elements are to remain elastic during an entire seismic event. These elements are called capacity protected elements. The inelasticity is forced to form in the predefined locations which have sufficient ductility. These damage locations in bridges are located at the ends of columns (forming plastic hinges). In the SDCL steel bridge system, the integral connection of the superstructure and substructure causes the damage location to be at the end of the column near cap beam.

In the initial stages of the numerical study, several connection details were considered. Following preliminary analysis of these connections, one of them was chosen for further development (Taghinezhadbilondy, 2016). Developing design provisions for any connection involves identifying failure modes associated with the connection. An ideal approach would be to subject many prototype bridges to series of ground motions and investigate the force transfer mechanism and failure modes associated with each element of the connection. Alternatively, one could carry out well designed experimental work and identify the failure modes and types of forces associated with various elements of given connection. However, this is very expensive and very time consuming. In this study, the behavior of the selected connection was investigated using detailed nonlinear finite element analysis and subjecting the connection to three types of loadings as described below. This approach was selected, partly because of the experiences gained by the authors during development of the SDCL system for non-seismic application (please see references listed above) and availability of calibrated non-linear finite element models, developed during previous investigations.

The numerical model consisted of middle pier and length of superstructure on either side of the pier to about the point of inflection (zero moment under dead load). The length of girders to either side of the middle of the pier was 4.3 m. The ends of girders, as shown in Figure 4, were connected over the pier using concrete diaphragm and the selected connection, which will be described later. The prototype bridge was a two span bridge, with each span being 28.95 m (95 ft). The cantilever ends of the girders in the numerical model, as shown in Figure 5, were subjected to three loading types as follows:

A) Push-down loading, simulating the gravity type loadings, to approximately comprehend the types of forces that connection elements would experience under gravity loads;
B) Push-up loading, simulating the vertical component of the seismic loads, to approximately comprehend the types of forces and failure modes that connection elements would experience under vertical components of ground motions during seismic events; and
C) Reversal loading, simulating the types of loading associated with longitudinal component (parallel to traffic flow) of the seismic loads, to approximately comprehend the types of forces and failure modes that connection elements would experience under horizontal components of ground motions during seismic events.

The connection selected to join the ends of the girder over the pier is shown in Figure 4. It should be noted that superstructure, including the selected detail and concrete diaphragm are capacity protected and must remain elastic during entire seismic event

Readers are referred elsewhere (Taghinezhadbilondy, 2016) for a detailed description of the numerical work leading to development of the connection shown in Figure 4 and identifying the function of each connection element during a major seismic event. The following section provides a brief description of the different elements of the proposed connection and their function for ABC application of an SDCL steel bridge system in high seismic areas.

- ***Tie bars and shear studs on the compression flange (identified as (1) in Figure 4)*** - This part of the proposed detail is the main difference between the details for non-seismic and seismic application of SDCL. These ties are to accommodate possible tension forces between the girders' bottom flanges. The tension may occur under positive moment, in the pier area, resulting from high vertical seismic excitations. The area of tie bars should be designed to resist a positive moment induced by 25% of the weight of the structure acting upward.

- ***Steel blocks at the end of the compression flanges (identified as (2) in Figure 4)*** - These blocks are used to pass the compression forces between the girders' bottom flange. This compression force is generated by superimposed dead and live load negative moment. The width of the block is equal to the width of the bottom flange, and the height of it is suggested by the previous work to be one-sixth of the height of the girder. The block size should be checked for negative moment generated from governing live load combination, the resulting moment arm is the distance between deck tension reinforcement and the center of steel blocks. The blocks are welded to the end of the compression flanges.
- ***End stiffeners (identified as (3) in Figure 4)*** - The stiffeners from the non-seismic version of the SDCL connection had to be modified for placing the tie bars between the compression flanges. These stiffeners, stiffen the webs at beam end against vertical buckling and provides smoother transfer of forces from beam to concrete diaphragm over the middle pier, when beam ends are subjected to positive or negative moments.
- ***Dowel bars (identified as (4) in Figure 4) -*** These reinforcements, similar to available detail for integral bent caps, are designed for the torsion and shear in bent cap. Torsion and shear in the bent-cap occurs under longitudinal (along traffic) excitations, and load transfer from girders to columns. These bars are also the main mechanism to resist the forces developed as a result of moment reversal during longitudinal component of the ground motion (parallel to traffic flow). Results of numerical studies indicated that the design of

dowel bars could be based on established Caltrans (Caltrans 2010) design provisions for capacity protected elements (Taghinezhadbilondy, 2016).

- ***Live load continuity reinforcement (identified as (5) in Figure 4) -*** These reinforcements are placed to provide the continuity for live and superimposed dead loads. The live load continuity deck reinforcement is incorporated in the deck design. In ABC application of SDCL, the deck reinforcement needs to be developed in the diaphragm. One approach is by hooking then inside the concrete diaphragm as shown in Figure 3.

The global and local behavior of the numerical model under push-down loading was same as non-seismic detail (Azizinamini, Yakel, and Farimani 2005). Under push-up loading, finite element results showed that continuity of bottom flange increases ductility and capacity of the connection. Since the bottom flange was not continuous, tie bars helped the system to increase the ultimate moment capacity. Under reversal loading, dowel bars were the most critical elements of the connection. The results demonstrated that tie bars over the bottom flange were unable to provide additional moment capacity for the system under moment reversal type loading. However, increasing the volume ratio of dowel bars can increase the moment capacity and prevent premature failure of the system under moment reversal, associated with along the traffic component of the ground motion.

Based on the above mentioned details, component level testing was performed at Florida International University (FIU). The main objective of the project was design and verification testing of a component level specimen using SDCL for seismic areas. If designed properly, the failure should not occur within the connection itself. Also, one of the objectives of the component testing was to verify the performance of the suggested detail before carrying out the shake table test. This project was a joint investigation between FIU and University of Nevada-Reno (UNR).

FIU was responsible for developing the detail for extending the application of the SDCL steel bridge system to high seismic areas, followed by a shake table test of a scaled two span steel bridge system incorporating the FIU detail.

Experimental Program

This section provides details of an experimental testing program for verifying the recommendations of numerical studies. A prototype two-span steel I-girder bridge was selected for finding the demand side of the detail over the pier under seismic loads. The prototype bridge was designed and scaled down to one-third for the purpose of this research. The scaled down bridge was designed to undergo the same stresses as the prototype bridge.

The prototype bridge had two 28.96 m (95 ft) spans with 9.75 m (32 ft) width and was designed based on AASHTO provisions (AASHTO, 2012). The superstructure consists of four W40x215 steel I-girders and a 19 cm (7.5 in.) deck. Simply supported end abutments and a middle pier bent supported by two columns were assumed for this bridge. In this research, for the purpose of component testing, a pier bent column and girders on both sides were considered in an inverted test setup.

Column

The column was designed to sustain large inelastic deformations prior to failure. Caltrans specifies target upper limits of displacement ductility to reduce demand imparted to capacity protected element (Caltrans 2010). Thus, the longitudinal reinforcement of scaled down column and volumetric ratio and spacing of spirals were designed in order to meet seismic provisions. As a result of scaling down, the size of the prototype column was scaled while the reinforcement ratio was kept constant. An axial load of 418 kN, assumed to be 10% of the product of gross cross-section area and concrete compressive strength, was applied to the column. The length of the column, from face of the cap beam to the line of action of lateral load, was 1.63 m (64 in.). The lateral load is applied to the connection through a rectangular cap at the end of column.

Girders and Deck

The superstructure was designed as simply supported for the dead loads of deck concrete and steel girders, and as continuous girders under live loads and superimposed dead loads. The W40x215 steel I-girders were scaled down to A709 GR50 steel plate girders, with 45.7 cm by 0.95 cm (18 in. by 0.375 in.) web and 15.2 cm by 1.59 cm (6 in. by 0.625 in.) flanges. The deck was scaled down to 7.6 cm (3 in.) thickness with #4 Grade 60 reinforcing bars at 12.7 cm (5 in.) spacing. The composite action between girder and deck was achieved through providing four 1.9 cm (0.75 in.) diameter shear studs, spaced at 45.7 cm (18 in.) on center. The details of the superstructure are shown in Figure 6.

Cap Beam and Connection

The capacity design approach was used for the cap beam and different details, based on seismic design provisions (Caltrans 2010; AASHTO 2011; AASHTO 2012). The entire concrete diaphragm connecting the girders with pre top deck over the pier was assumed to be the capacity protected element and was designed to remain elastic in accordance with the specifications listed above. The connection between superstructure and substructure was assumed to be monolithic, forming a frame action. As a result, under longitudinal excitation (parallel to traffic) column deformations result in double curvature, and under transverse excitation column deformations result in single curvature or double curvature as shown in Figure 7.

The prototype bridge used for this project had a two-column bent in the middle pier, so the bent cap was designated and designed as capacity protected element in both directions. This approach guarantees the superstructure has enough strength to remain elastic under transferred forces from the column at the ultimate load level. The expected nominal capacity and the level in which the capacity protected element remains elastic were calculated using moment curvature and finite element analysis and were compared to over-strength capacity of the column. This procedure is suggested by Caltrans, in which the over-strength capacity of the column is the nominal capacity of the column increased by 20%. Figure 8 shows the calculated over-strength capacity of the column and capacity of the bent cap in both directions.

After designing the cap beam and diaphragm based on the capacity approach, different details of the bent cap, vertical bars (dowel), horizontal bars, side bars, etc., were designed and checked according to Caltrans procedures. The cap beam, designed as a whole, consisted of 20.3 cm by 61.0 cm (8 in. by 24 in.) dropped cap, 48.3 cm by 61.0 cm (19 in. by 24 in.) diaphragm, and 7.6 cm (3 in.) deck. The final dimensions of the bent cap were 76.2 cm by 61.0 cm (30 in. by 24 in.), shown in Figure 9. As mentioned above, the dropped cap section (8 in. by 24 in. section) was designed to support the weights of steel girders, deck concrete weight and construction loads, before casting the concrete diaphragm over the pier. Details of bent cap and column reinforcements are shown in Figure 9.

The elements of the suggested SDCL detail for high seismic regions for the test specimen, were designed based on the detailed finite element analysis described elsewhere (Taghinezhadbilondy, 2016) and resulted in the following details:

- ***Tie bars between the shear studs on the compression flange (identified as 1 in Figure 4)* -** Two U-shaped #3 bars on each side of each girder between two 1.9 cm (0.75 in.) diameter shear studs on each compression flange. The total area of tie bars should be designed based on a positive moment induced by 25% of weight of the structure acting upward.
- ***Steel blocks at the end of the compression flanges (identified as 2 in Figure 4)* -** 5.1 cm by 5.1 cm by 15.2 cm (2 in. by 2 in. by 6 in.) steel block welded to the compression flange. The sizing of these steel blocks was based on previous work for development of SDCL detail for non-seismic regions. Based on the recommended design provision, the size of the steel block should be as follows: the width of the block should be equal to the width of the bottom flange and the height of it equal to one-sixth of the height of the girder.
- ***End stiffeners (identified as 3 in Figure 4)* -** Two 1.3 cm plates, welded to the web and tension flange, 10 cm to the end of each girder. It is recommended that the thickness of end stiffeners be equal to or more than the thickness of the web. The height of the web stiffeners should be based on detailing to accommodate the placement of tie bars.
- ***Live load continuity reinforcement (identified as 5 in Figure 4)* -** The live load continuity is achieved by placement of the longitudinal (parallel to traffic flow) reinforcement in the deck. The design of this reinforcement is based on the negative moment, over the pier, developed by governing live load combination. For the test specimen, 10 #4 bars were provided in the deck. In the ABC application, to develop these reinforcement, the end of the reinforcement was hooked in the concrete diaphragm with 90° hook, as shown in Figure 4.

Test Setup

The results of numerical study indicated that the behavior of the SDCL connection is more critical under along-traffic excitations. In the case of an integral bridge, the longitudinal component of earthquake load results in a double curvature deformation with the inflection point at the middle of the column (Figure 10), when column ends are fixed. The length of the superstructure is taken between inflection points of two adjacent spans, created by placement of uniform load over the two spans. Similarly, the length of column represents the location of inflection point. After a thorough review of various test setups, used in previous similar investigations (Wassef et al., 2004; Patty, Seible, and Uang, 2001; Snyder et al., 2011) an inverted test set up as shown in Figure 11 was selected for experimental investigation. In the inverted setup used, the ends of the girders were simply supported and lateral load was applied to the end of the column.

The length of the test specimen was adjusted to approximately account for the fact that inverted test setup caused an additional negative moment in the pier due to dead weight of the specimen. Figure 10 and Figure 11 show the test setup and resulting shear and moment diagrams. The application of axial compressive load to column, created by dead weight of the structure was achieved by using threaded bars as shown in Figure 11. The lateral load was applied using a hydraulic actuator to the cap on top of the column, reacting to a frame fixed to the strong floor. The test setup was instrumented with string pots, load cells, strain gauges, potentiometers and pressure transducers.

Construction and Material Properties

Following the proposed inverted test setup, the concrete was cast in three stages: 1) casting deck up to the girder flanges, 7.6 cm (3 in.); 2) casting cap beam and diaphragm up to the column, 68.6

cm (+27 in.); and 3) casting the column and loading cap, 213.4 cm (+84 in.). The specimen dimensions and the constructions steps are shown in the Figure 12. In the ABC application of the SDCL system, first a dropped cap beam is placed over the columns, followed by casting the concrete diaphragm to join the pre-topped girders over the pier. This two-step process forms a cold joint between two layers of concrete. A surface preparation in the field is required for the dropped cap beam and concrete diaphragm to work monolithically. In the construction of test specimen dropped cap bean and concrete diaphragm were constructed in one step (stage 2).

Concrete samples were taken during each stage of construction. The concrete cylinders were tested for compression one day after the completion of cyclic tests. The average concrete compressive strength for stages 1-3 was 58.6 MPa, 55.8 MPa, and 36.0 MPa respectively. The reinforcing steel used were Grade 60 ASTM A706 bars in three sizes of #3, #4 and #5, with average yield stress of 469 MPa and ultimate stress of 779 MPa.

Test Procedure

The specimen was loaded axially through threaded bars as shown in Figure 11. This axial load was kept constant while subjecting the column to cyclic lateral load. The level of axial load applied was about 10% of pure axial load capacity of column, calculated as follows;

$$P = A_g f'_c$$

Where

A_g : Gross cross-section area,

f'_c : Specified concrete compressive strength.

The specimen was subjected to cyclic lateral loading in a sequence similar to Figure 13. This pattern was not intended to represent any specific earthquake. Nevertheless, experiences show that structural elements surviving such loading in the laboratory tests, while providing set levels of ductility, have provided good performances during major seismic events.

Displacement-control cyclic loads with increments of first yield displacement Δ_y, were applied to the column until failure. The first yield displacement of the column was calculated during the first cycle, schematically shown in Figure 14. In this cycle, the specimen was loaded to about twice the analytical yield displacement. The first yield displacement was calculated based on initial stiffness and maximum load applied.

Three cycles at each displacement ductility level, multiples of first yield displacement, was applied to the specimen. The loading was stopped when lateral load capacity of the column decreased significantly (more than 20%). Displacement ductility at each cycle is defined by ratio of maximum lateral displacement to first yield displacement Δ_y (Figure 13).

Test Observations

The observed damages at the end of each third cycle at different displacement ductility ratios are shown in Figure 15. The first cracks were seen during the first cycle on the column in the plastic hinge region. First signs of crushing in the cover concrete were also observed during the first cycle. It is believed that this behavior occurred because the specimen was subjected to load levels causing yielding of column reinforcement during the first cycle to establish the first yield displacement. Most of the observed cracks were in the plastic hinge region of the column. Cover concrete started to spall at displacement ductility ratio of 2. The spalling was extended to larger areas on later stages, but was limited to the expected plastic hinge region.

Limited superficial cracking was observed on the cap beam near the column on both sides. The first crack on the cap beam formed at displacement ductility ratio of 3. By the end of the test, few cracks were observed on either side of the cap beam as shown in Figure 16. The cracked concrete was removed after the test and depth of cracking was estimated to be less than 5 cm, and only limited to the cap beam cover concrete. The main reason for limited cracking in the cap beam is believed to be a result of scaling. The minimum bent cap width suggested by Caltrans is 61 cm (2 ft) larger than column diameter. The scaling down of the connection resulted in a cap beam 20 cm wider than column diameter (4 in. on each side). This reduced width is insufficient for joint shear transfer and thus believed to be the reason for cracking on the cap beam. During the test, the diaphragm and the deck remained intact without any visible cracks or yielding.

Mode of Failure

The specimen was able to resist three cycles at displacement ductility ratio of 6 (6.5% drift). In the last cycle of displacement ductility ratio of 6, the longitudinal reinforcement on both sides of the column exhibited signs of buckling. As the testing regime was continued to displacement ductility ratio of 7, the longitudinal reinforcement on one side of column fractured. This rebar fracture resulted in a 20% strength reduction and the testing was halted. The hysteresis loops did not show any strength degradation before the fracture of rebar.

Test Results and Discussion

The resulting lateral load vs. lateral displacement and the moment curvature as obtained from test are shown in Figure 17 and Figure 18, respectively. Figures 17 and 18 also show results as obtained from moment curvature analysis, demonstrating good agreement with test results. The overall behavior of the specimen was symmetrical.

The distribution of peak tensile strains on column longitudinal reinforcement during each displacement ductility ratio is plotted in Figure 19. As shown in Figure 19, the strain in the longitudinal reinforcement, within 5 cm below the face of cap beam, experienced strains exceeding yield strain. However, at about 20 cm below the cap beam face, strains are well below the yield strain.

The strain measurements on the vertical legs of closed stirrups within the concrete diaphragm, or as it referred to as dowel bars in this paper, as shown in Figure 20, validates the fact that the cap beam and diaphragm remained elastic during the test. The maximum measured strain on the vertical legs of the dowel bars was 900 micro-strain, as indicated in Figure 20.

Measurements on the tie bars (Element 1 in Figure 4) showed a gradual increase in the strains during the test. Maximum strain observed in the tie bars during entire loading cycles was 300 micro-strain. These results from dowel bars and tie bars verified the aforementioned conclusion from the numerical results, that the dowel bars play the main role under along-traffic excitations (reversal loading).

The distribution of maximum tensile strains in the longitudinal reinforcement in the deck during displacement ductility ratio of 6 is shown in Figure 21. As shown in this figure, the observed maximum tensile strains in the longitudinal reinforcement was 205 micro-strain, well below the yield strain.

The curvature distribution along the height of the column is show in Figure 22. These curvatures were extracted from the strain measurements, made using potentiometers attached to column. The results, as expected, show higher curvatures close to the cap beam, due to a higher level of damage in the section.

The column was able to sustain three cycles at displacement ductility ratio of 6 and failed during the first cycle of displacement ductility ratio of 7. Therefore, the displacement ductility capacity of the column was concluded to be 6 without any observed strength degradation. Strains in the cap beam, tie bars and deck show that the suggested SDCL connection detail remained elastic at ultimate load level.

Conclusions

This paper presents a detail capable of extending the application of the SDCL steel bridge system to high seismic areas. The development of detail was mainly based on numerical studies. To verify the merits and performance of the suggested detail, tests were carried out on a scaled test specimen. The design approach used was capacity design, where cap beam and superstructure must remain elastic, while plastic hinge is only allowed to form at the end of columns, during major seismic event. The test specimen was instrumented to measure the levels of strains in various elements of the detail and verify if capacity protected elements remained in elastic region, while plastic hinge formed at the end of the column. Test results verified that the suggested detail is capable of meeting the intents of capacity protected design provisions as stated in Caltrans specification. The plastic hinge formed at the end of the column, as designed. The capacity protected elements remained in elastic region, while the column provided a displacement ductility level of 6 before failing. Failure was by fracture of longitudinal reinforcement in the column and within the plastic hinge regions.

This project is a joint project between Florida International University (FIU) and the University of Nevada-Reno (UNR). FIU is responsible for developing the detail that is capable of extending the application of SDCL steel bridge system to high seismic areas. It was decided to carry out the component testing on the suggested FIU detail before conducting planned shake table test on a one-third scale of a two-span steel bridge and incorporating the FIU detail. As documented in this paper, the suggested detail can provided the intended function. The next step will be conducting the shake table test at UNR.

Acknowledgments

This project is supported by the U.S. Department of Transportation through the Accelerated Bridge Construction University Transportation Center (ABC-UTC) at Florida International University as lead institution and Iowa State University, University of Nevada-Reno, University of Washington, and University of Oklahoma as partner Universities. The opinions, findings and conclusions expressed here are those of the author(s) and not necessarily of the sponsor.

References

AASHTO. (2011). "Guide Specification for LRFD Seismic Bridge Design," American Association of State Highway and Transportation Officials, Washington, D.C.

AASHTO. (2012). “LRFD Bridge Design Specifications.” American Association of State Highway and Transportation Officials, Washington, D.C.

Azizinamini, A. (2014). “Simple for Dead Load-Continuous for Live Load Steel Bridge Systems.” *Engineering Journal-American Institute of Steel Construction,* 51 (2), 59–81.

Azizinamini, A., Yakel, A., and Farimani, M. (2005). “Development of a Steel Bridge System : Simple for Dead Load and Continuous for Live Load.” *NDOR Research Project,* P542.

Caltrans, S D C. 2010. “Caltrans Seismic Design Criteria Version 1.6.” California Department of Transportation, Sacramento, CA.

Farimani, R., Javidi, S., Kowalski, D. and Azizinamini, A. (2014). "Numerical Analysis and Design Provision Development for the Simple for Dead Load – Continuous for Live Load Steel Bridge System." *Engineering Journal-American Institute of Steel Construction*, 51(2), 109-126.

Javidi, S., Yakel, A., and Azizinamini, A. (2014). "Experimental Investigation, Application and Monitoring of a Simple for Dead Load-Continuous for Live Load Connection for Accelerated Modular Steel Bridge Construction." *Engineering Journal-American Institute of Steel Construction*, 51(3), 177-198.

Lampe, N., Mossahebi, N., Yakel, A., Farimani, R., and Azizinamini, A. (2014). "Development and Experimental Testing of Connections for the Simple for Dead Load-Continuous for Live Load Steel Bridge System." *Engineering Journal-American Institute of Steel Construction*, 51(2), 83-108.

Patty, J., Seible, F., and Uang, C. M. (2001). *Seismic Response of Integral Bridge Connections*. (No. SSRP-2001/16)

Snyder, R., Vander Werff, J., Thiemann, Z., Sritharan, S., and Holombo, J. (2011). "Seismic Performance of an I-Girder to Inverted-T Bent Cap Connection." *Reports and White Papers*.

Taghinezhadbilondy, R. (2016). "Extending Use of Simple for Dead Load and Continuous for Live Load (SDCL) Steel Bridge System to Seismic Areas."

Wassef, W. G., Davis, D., Sritharan, S., Vander Werff, J. R., Abendroth, R. E., Redmond, J., and Greimann, L. F. (2004). *Integral steel box-beam pier caps* (No. Project C12-54 FY'99).

Yakel, A., and Azizinamini, A. (2014). "Field Application Case Studies and Long-Term

Monitoring of Bridges Utilizing the Simple for Dead-Continuous for Live Bridge System." *Engineering Journal-American Institute of Steel Construction*, 51(3), 155-175.

Figures

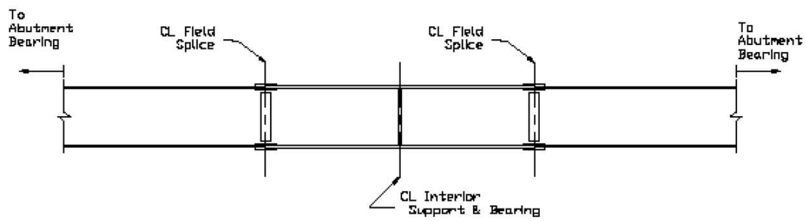

Figure 1 Conventional two-span continuous bridge girder (Azizinamini 2014).

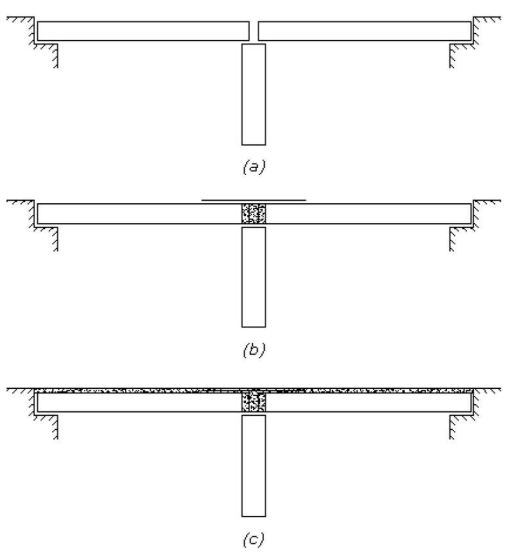

Figure 2 Construction sequence for SDCL bridge system (Azizinamini 2014).

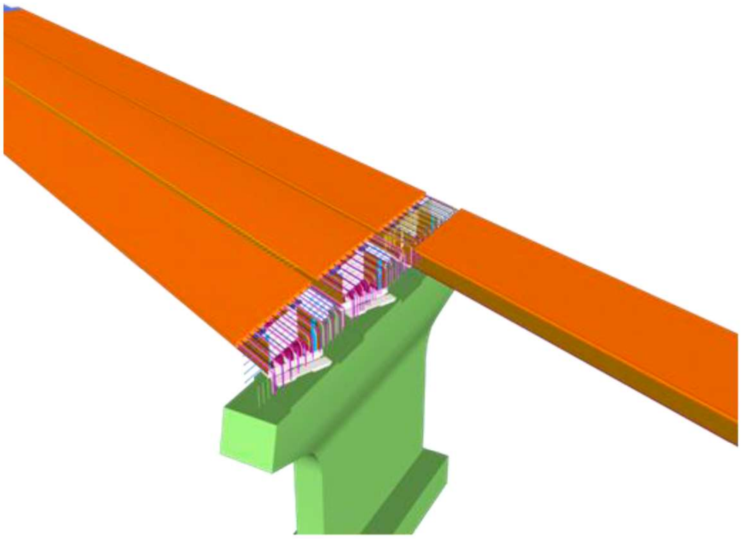

Figure 3 ABC application of SDCL in non-seismic areas (Azizinamini 2014).

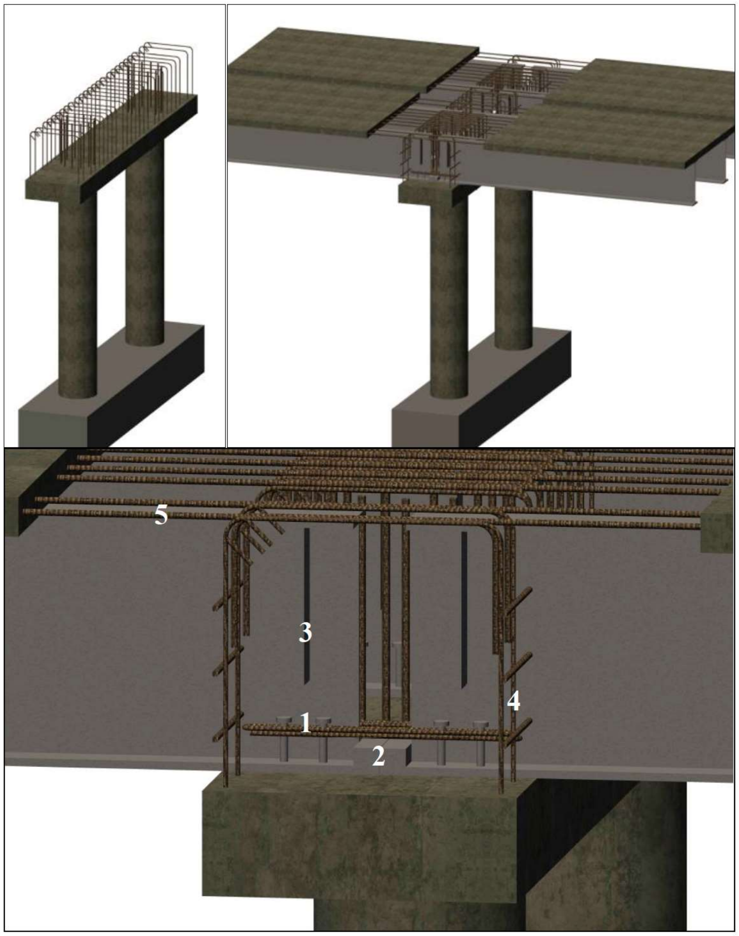

Figure 4 Schematic view of developed SDCL connection details for seismic areas.

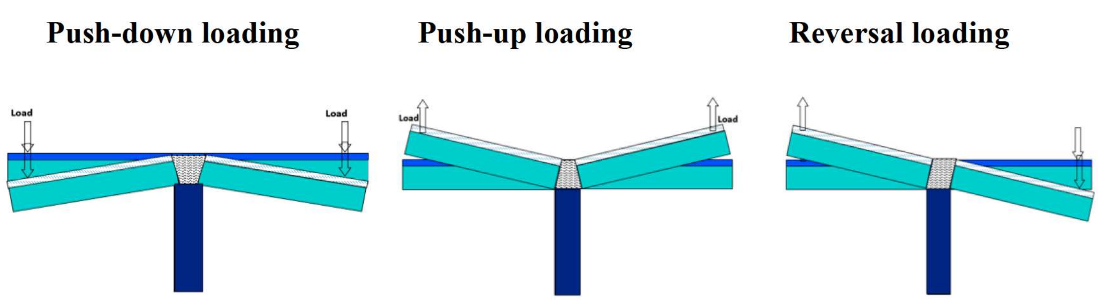

Figure 5 Three types of loading subjected to numerical models (Taghinezhadbilondy 2016).

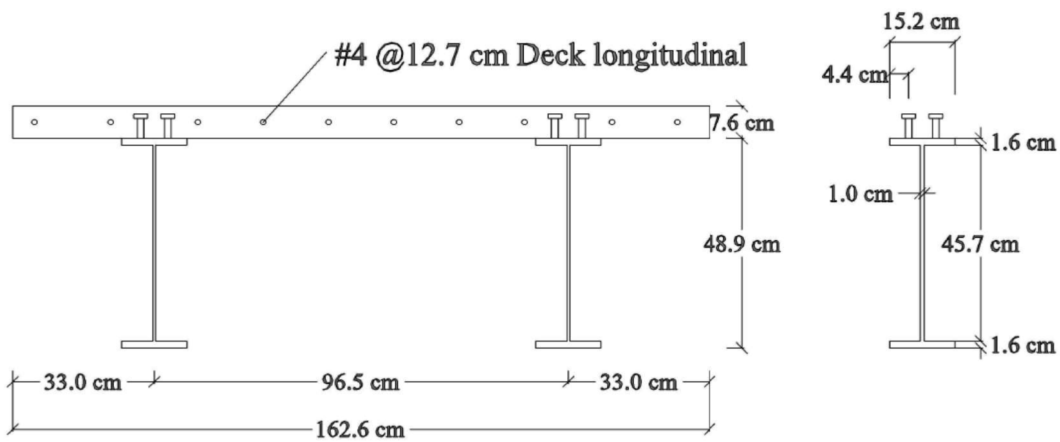

Figure 6 Test specimen superstructure details (one-third scale).

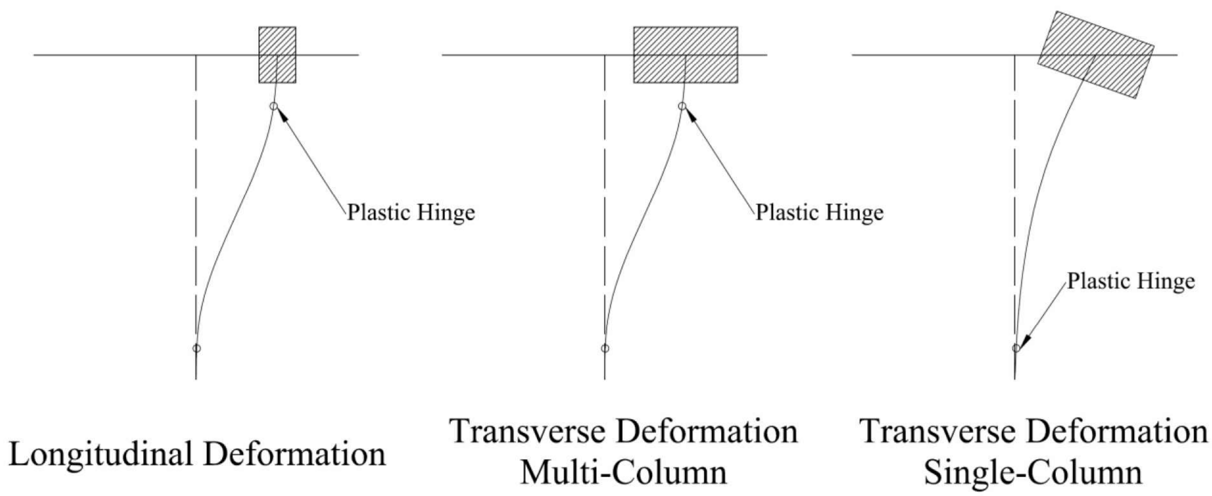

Figure 7 Deflected shape of pier column in longitudinal and transverse directions.

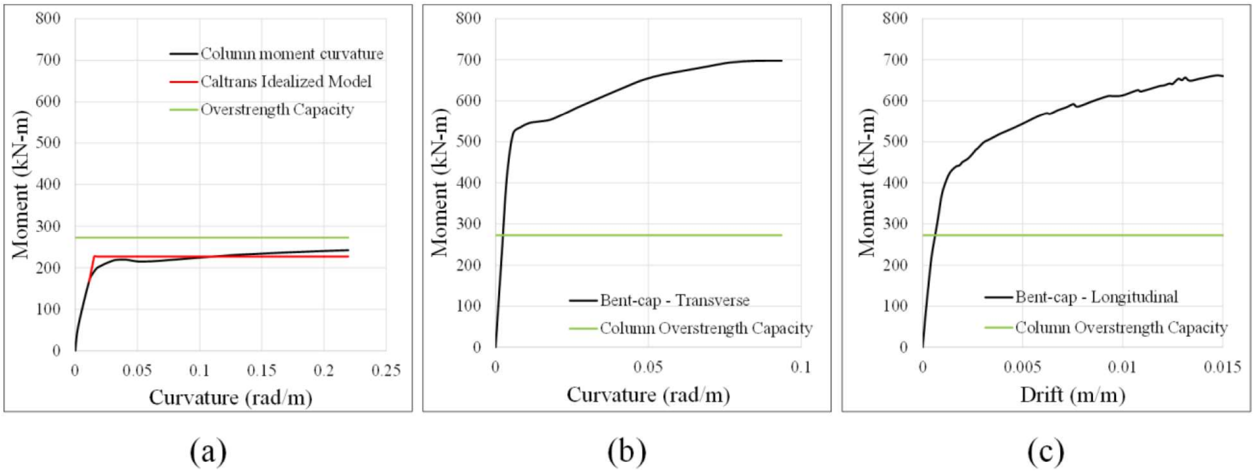

Figure 8 (a) Column moment-curvature and computed overstrength capacity, (b) Bent cap moment-curvature in transverse direction compared to column over-strength capacity, (c) Bent cap moment-drift in longitudinal direction (from FE analysis (Taghinezhadbilondy 2016)) compared to column overstrength capacity.

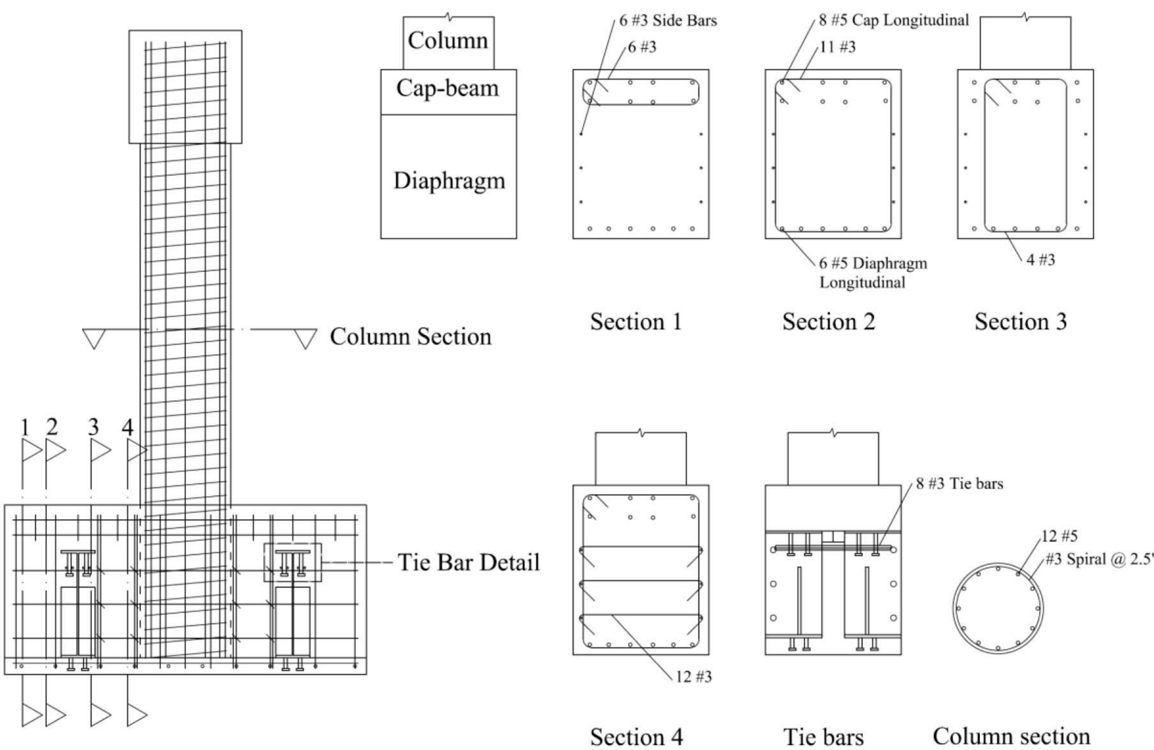

Figure 9 Bent cap and column reinforcement details.

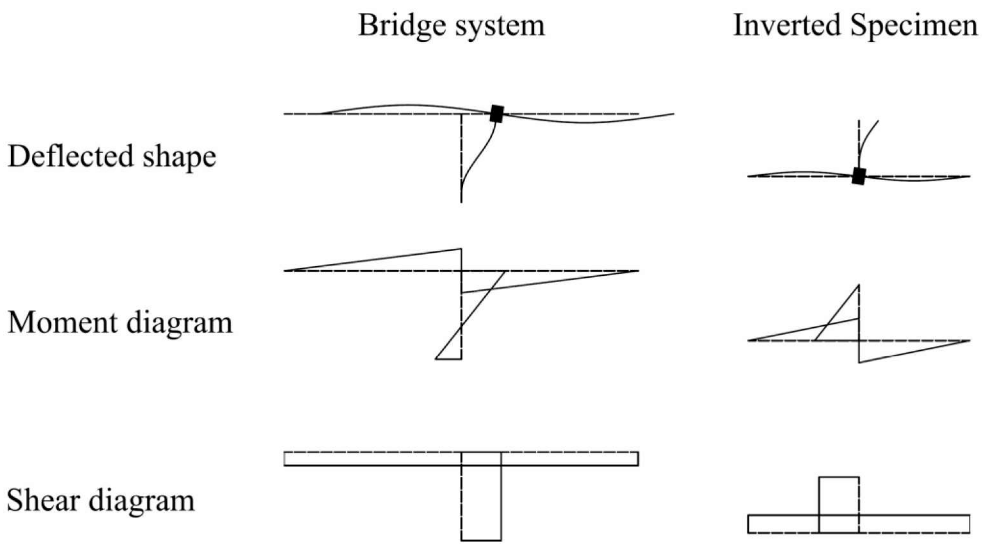

Figure 10 Deflected shape, moment diagram and shear diagram of bridge system and inverted specimen under longitudinal excitations.

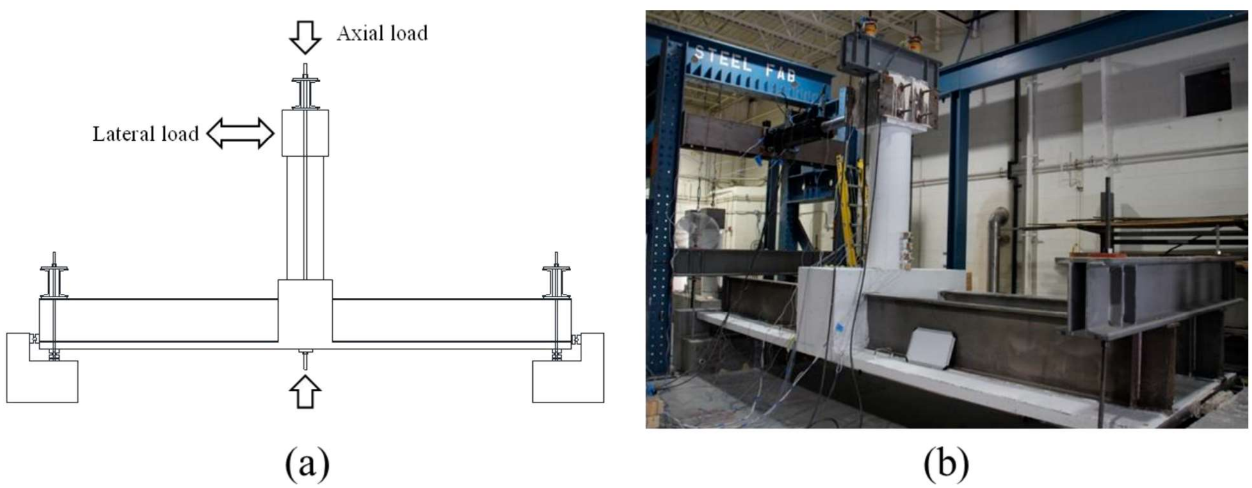

Figure 11 (a) Test setup simulating the actual structural behavior, (b) SDCL test specimen constructed in FIU structures lab.

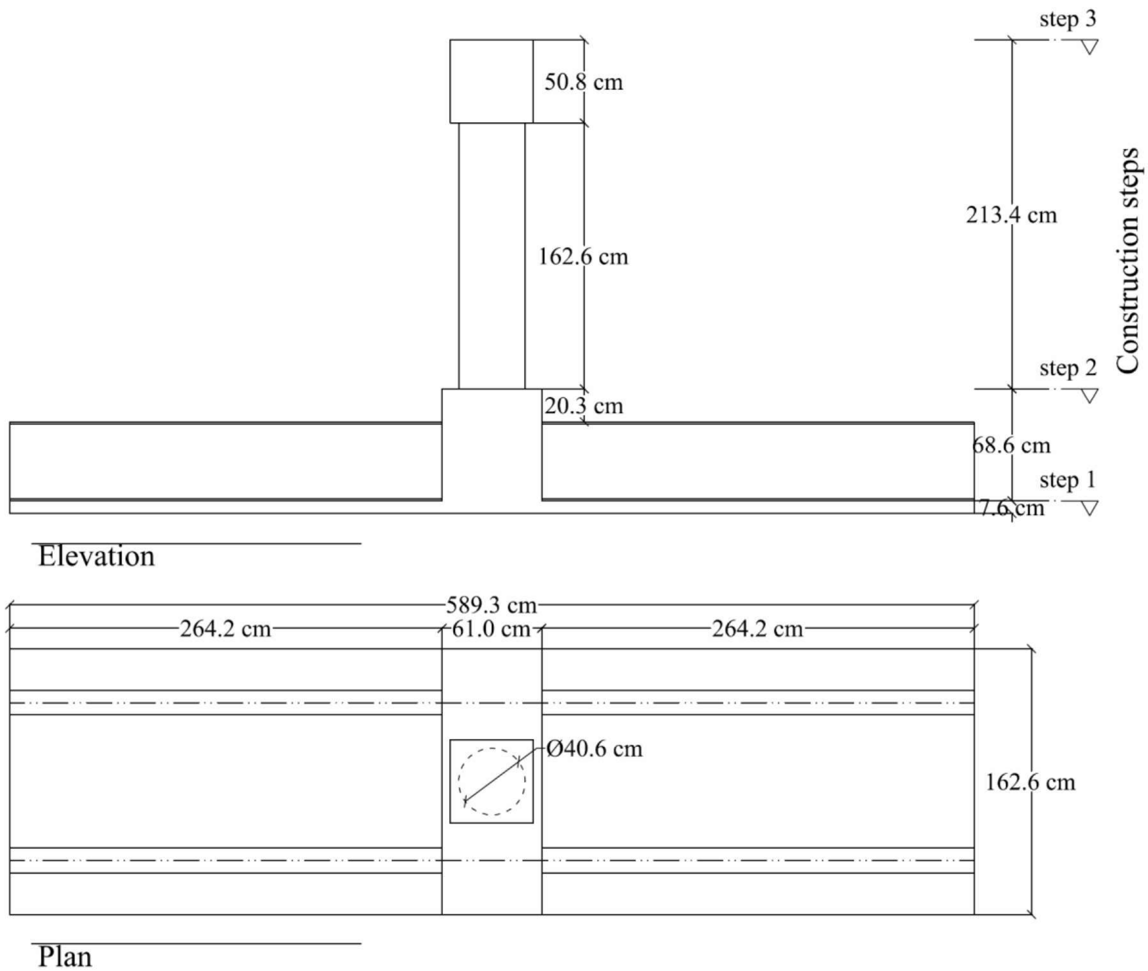

Figure 12 Details and dimentions of the test specimen.

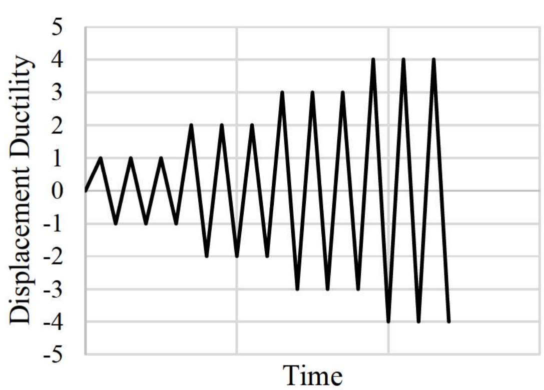

Figure 13 Loading schedule for lateral load.

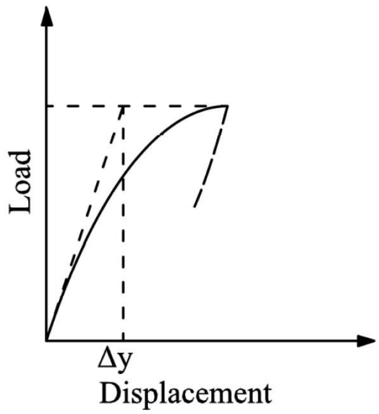

Figure 14 Experimental definition of first yield displacement.

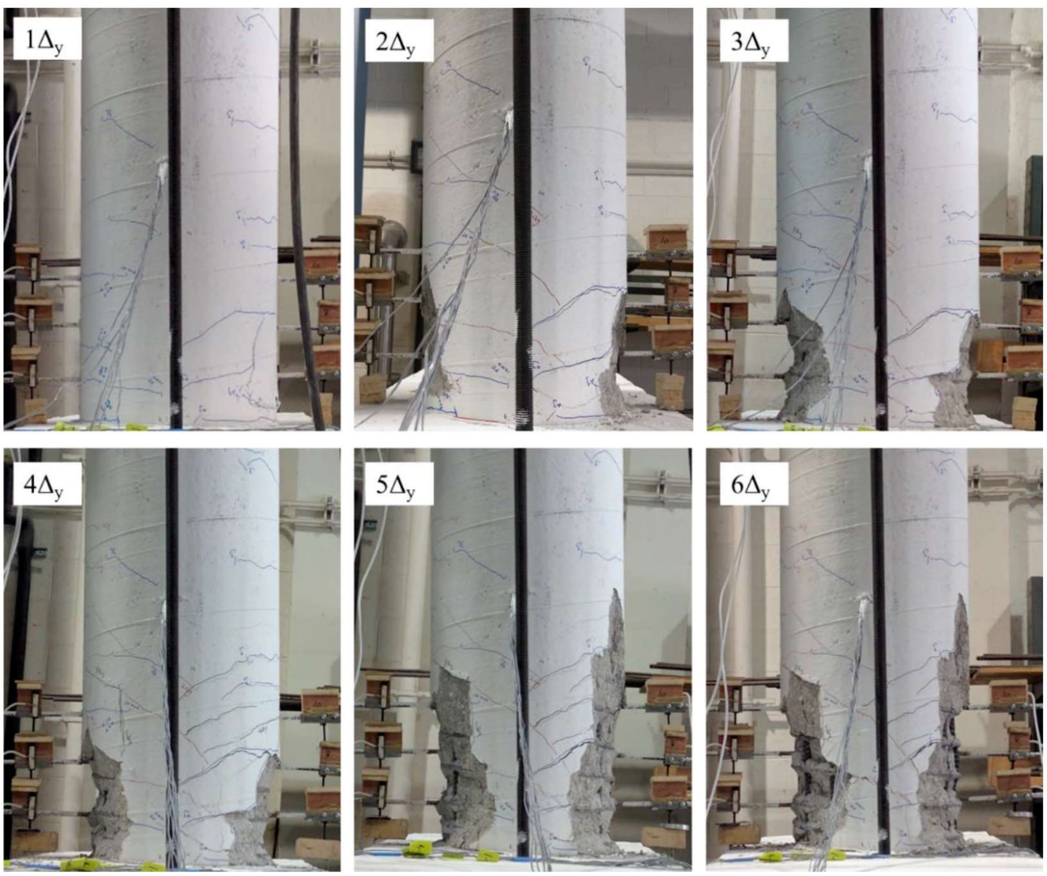

Figure 15 Observed damage in the plastic hinge region at different levels of test.

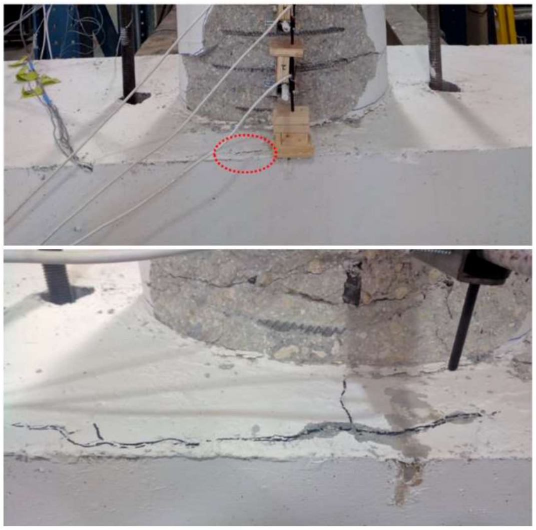

Figure 16 Crack formation on the cap beam.

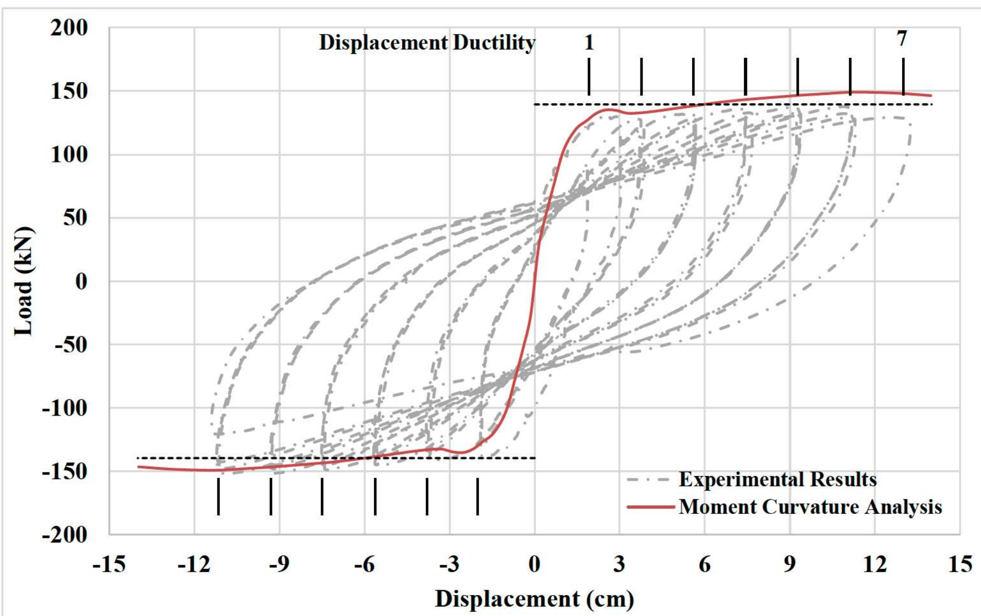

Figure 17 Experimental load-displacement response.

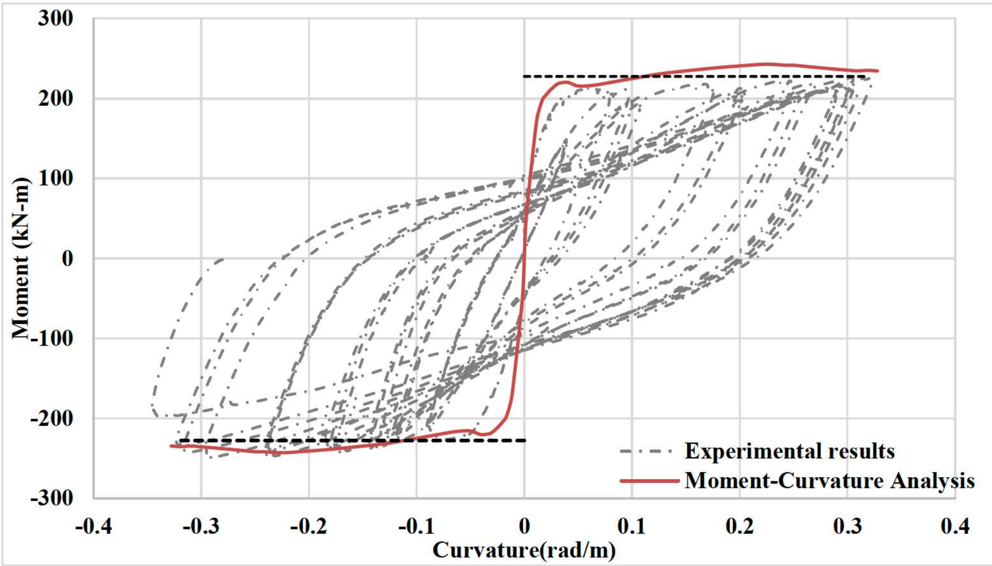

Figure 18 Experimental moment curvature at column base.

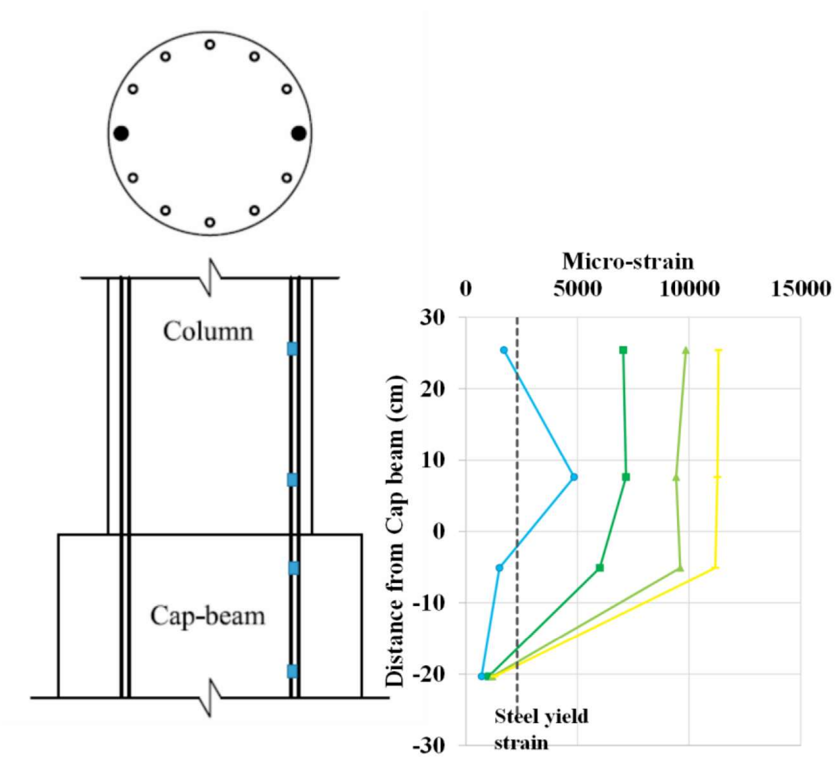

Figure 19 Strain measurements on column longitudinal reinforcement.

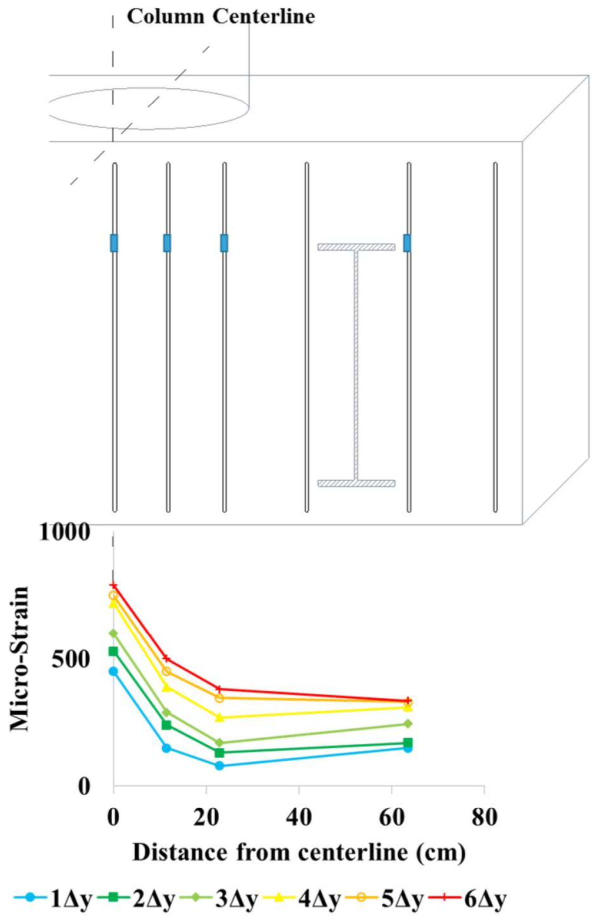

Figure 20 Strain measurements on dowel bars.

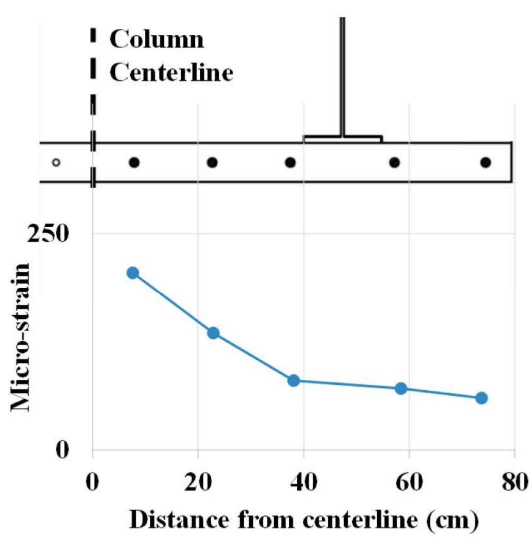

Figure 21 Strain measurements on deck longitudinal reinforcement.

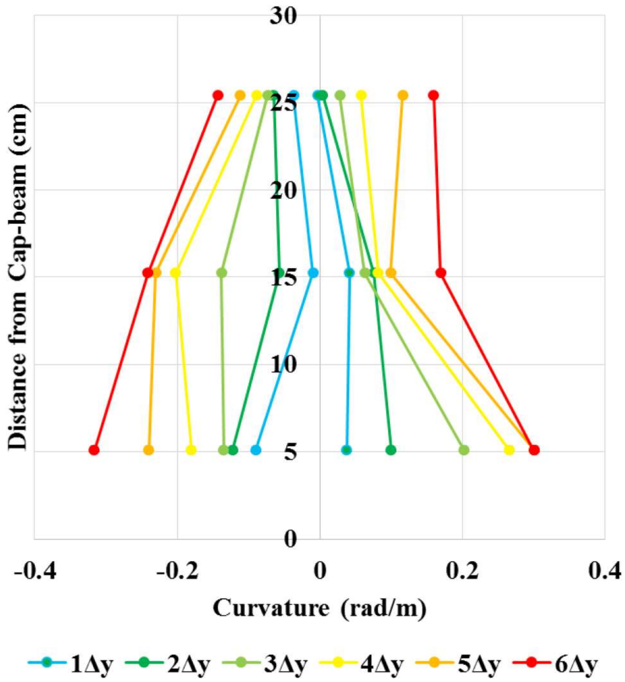

Figure 22 Plastic hinge curvature profile.